Natural Underwater Adhesives

Russell J. Stewart, Todd C. Ransom,† Vladimir Hlady

Department of Bioengineering, University of Utah, Salt Lake City, Utah 84112

Correspondence to: R. J. Stewart (E-mail: rstewart@eng.utah.edu)

Received 10 January 2011; revised 28 March 2011; accepted 28 March 2011; published online
DOI: 10.1002/polb.22256

ABSTRACT: The general topic of this review is protein-based underwater adhesives produced by aquatic organisms. The focus is on mechanisms of interfacial adhesion to native surfaces and controlled underwater solidification of natural waterborne adhesives. Four genera that exemplify the broad range of function, general mechanistic features, and unique adaptations are discussed in detail: blue mussels, acorn barnacles, sandcastle worms, and freshwater caddisfly larva. Aquatic surfaces in nature are charged and in equilibrium with their environment, populated by an electrical double layer of ions as well as adsorbed natural polyelectrolytes and microbial biofilms. Surface adsorption of underwater bioadhesives likely occurs by exchange of surface bound ligands by amino acid sidechains, driven primarily by relative affinities and effective concentrations of polymeric functional groups. Most aquatic organisms exploit modified amino acid sidechains, in particular phosphorylated serines and hydroxylated tyrosines (dopa), with high-surface affinity that form coordinative surface complexes. After delivery to the surfaces as a fluid, permanent natural adhesives solidify to bear sustained loads. Mussel plaques are assembled in a manner superficially reminiscent of *in vitro* layer-by-layer strategies, with sequentially delivered layers associated through $Fe(dopa)_3$ coordination bonds. The adhesives of sandcastle worms, caddisfly larva, and barnacles may be delivered in a form somewhat similar to *in vitro* complex coacervation. Marine adhesives are secreted, or excreted, into seawater that has a significantly higher pH and ionic strength than the internal environment. Empirical evidence suggests these environment triggers could provide minimalistic, fail-safe timing mechanisms to prevent premature solidification (insolubilization) of the glue within the secretory system, yet allow rapid solidification after secretion. Underwater bioadhesives are further strengthened by secondary covalent curing. © 2011 Wiley Periodicals, Inc. J Polym Sci Part B: Polym Phys 49: 757–771, 2011

KEYWORDS: adhesives; biomimetic; biopolymers

INTRODUCTION Without trying hard, dozens or more organisms could be identified in a clear-running mountain stream that use bioadhesives to support their aquatic lifestyle. Caddisfly larva would be prominent amongst them.[1] The majority of the caddisfly lifecycle is spent in the larval stage feeding below the surface of freshwater lakes and streams. After pupating underwater, they emerge as aerial adults to mate briefly and reinitiate the cycle. The feeding larvae make varied use of sticky underwater silk to exploit their habitats. Some live in stationary retreats constructed with sticky silk and gathered rocks, leaves, or sticks. The remarkable composite structures are often equipped with underwater silk webs to capture prey from water channeled through the retreat. Others species are mobile foragers, their soft abdomens protected by armored cases built by taping together small rocks with their sticky silk (Fig. 1). Some case-maker species build with sticks, or leaves, cut to size and assembled into species-specific shapes, from conical tubas to square clarinets.

The beach is likewise a smorgasbord of invertebrate animals glued to wet surfaces: mussels hang on with a handful of high-tech threads constructed to mitigate the mechanical mismatch between hard rock and soft invertebrate body,[2] armor-plated acorn barnacles glue calcareous base plates to rocks, pilings, and boat bottoms to the consternation of the maritime industry,[3] and sandcastle worms live in tubes assembled with sand, shell fragments, and dabs of underwater proteinaceous glue,[4] conjoined with other tubes into reef-sized sandcastles. Conus snails anchor precious egg capsules onto an adhesive base,[5] flagellated zoospores of brown algae (kelp) glue themselves to selected surfaces to begin the gametophyte stage of the lifecycle,[6] and starfish mosey along on temporary adhesive footprints.[7] The surfaces with no macroorganism inhabitants are covered with communities of microbes that have attached themselves in complex, biomacromolecule-structured biofilms.[8] Like aquatic macroorganisms, their reproductive success depends on stably positioning themselves in suitably resource-rich environments. There are other uncounted, unpublicized organisms that produce natural underwater adhesives; all have evolved separate and distinct working solutions for their particular underwater bonding requirements.

Humans could find many uses for effective underwater adhesives—attaching sensors, beacons, or ordnance under the

†Deceased.

Russell J. Stewart received his PhD in biochemistry from the University of California, Santa Barbara in 1989. After a postdoctoral fellowship at Harvard University, he worked at the Rowland Institute for Science in Cambridge, MA. In 1994, he joined the faculty of the Department of Bioengineering at the University of Utah. His long standing research interests are in biomimetic engineering. The current focus is development of medical adhesives for hard and soft tissue repair modeled after the natural underwater adhesives of sandcastle worms and caddisfly larva.

Todd C. Ransom was born in Princeton, New Jersey in 1982 and grew up in Orem, Utah. He graduated with honors from the University of Utah in May 2009 with a BS in biomedical engineering. After graduating, he worked at BD Medical in Salt Lake City, Utah. He passed away in July 2010.

Vladimir Hlady is a Professor of Bioengineering at University of Utah. He received B.S., M.S., and D.Sc. degrees in Chemistry from the University of Zagreb, Croatia. Before moving to University of Utah, he worked at the Institute "Rudjer Boskovic," Zagreb in the area of pathological mineralization. His current research focus is on the interactions of proteins at solid/liquid interfaces. He has two patents and published more than 120 scientific papers, reviews, and book chapters.

waterline, stopping watery leaks, and in medicine, repairing wet living tissues. Synthetic adhesives developed for dry applications perform poorly on wet surfaces, or under water. Adhesive technologists who have adapted cyanoacrylates, epoxies, and other synthetic adhesives for underwater applications may marvel at the numerous solutions to the problem of underwater bonding apparent in nature. On the other hand, those who have spent their careers trying to prevent proteins from sticking to medical implants in wet physiological environments may wonder "What wet adhesion problem?." Robust, nonspecific adsorption of proteins to clean wet surfaces is not rare in their experience and does not require unique proteins or special chemistries. Synthetic adhesives, even underwater, can have bulk cohesive strength much greater than natural underwater adhesives, but eventually fail due to poor interfacial adhesion in the presence of water.[9–11] Most proteins adhere strongly to wet interfaces, but generally in monolayers,[12] and are poor glues[13] when wet. Even natural protein-based underwater adhesives are not particularly impressive for their bond strength, a few hundred kP_a. Wilker's group found the tensile strength of mussel adhesive plaques (288 ± 110 kPa on Al) to be about 1/3 that of Elmer's white glue (polyvinylalchohol) and 1/30th that of household superglue (ethylcyanoacrylate).[14]

In overview, detailed discussion is limited to permanent underwater bioadhesives produced by a few paradigmatic species that well illustrate the diversity of function and chemistry of natural underwater adhesives, yet at the same time allow common features to be highlighted. Accounts of numerous other biological adhesives under study, aquatic and terrestrial, are available.[15–17] Effective underwater bonding requires robust interfacial adhesion to wet native surfaces with little, if any, surface preparation, deposition of the adhesive onto sites often completely submerged in water, and controlled solidification after deposition for sufficient cohesive strength to resist loading. Each of these aspects of underwater adhesion will be discussed.

INTERFACIAL CHEMISTRY: ADHESION

Native Surfaces

The major challenge of adhesive bonding is weak layers of contaminants between adhesive and adherend that prevent direct chemical contact.[18] Professional bonders, such as the engineers who glue cars and jets together, use energy intensive processes, such as plasmas and highly reactive chemical etchants, to create clean high energy surfaces. Interfacial adsorption of an adhesive reduces the surface energy of the adherend, which provides a driving force for adhesion. The problem of surface contamination is nowhere more acute than in natural aquatic environments. Unlike the high-energy surfaces in clean rooms and drawings, the surfaces of metal oxides, clays, and other minerals in water are populated with a varied mix of adsorbed ions, ionic complexes, organic polymers, and microbial biofilms. Interfacial forces create an electrical double layer, drawing ions into the tightly bound Stern layer and a diffuse outer ionic cloud. Free biopolymers

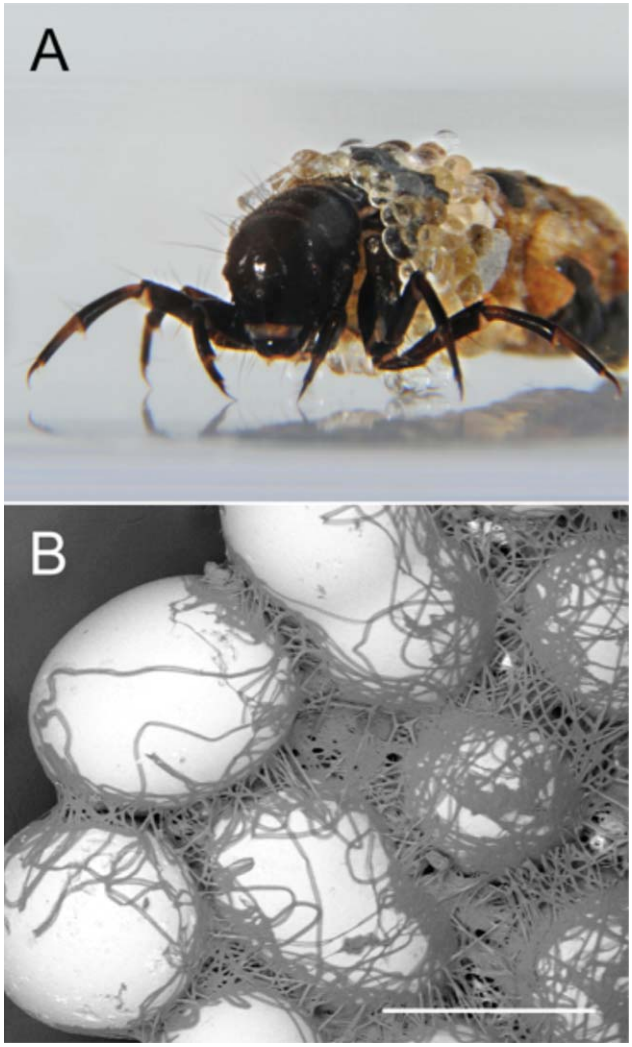

FIGURE 1 (A) Underwater caddisfly larva in case partially reconstructed with glass beads. (B) Scanning electron micrograph of inside of glass case. Adhesive silk stitches hold the case together. Scale bar = 500 mm. Photo credit University of Utah.

can adsorb on top of the ion-populated interface, and/or displace adsorbed ions. Accumulation of these species and continuous ion exchange processes lower the interfacial energy, creating a dynamic chase around an elusive equilibrium with minimal interfacial energy. These are the native surfaces on which aquatic organisms live or die.

How do underwater animals adhere to low energy native surfaces equilibrated with their immediate environment? There are two extreme scenarios: The animals "clean up" the surface by expending metabolic energy to chemically or physically remove the adsorbed layers to increase the interfacial energy for better adhesion. Or, natural bioadhesives are adapted to adhere to native low energy surfaces. The first scenario seems physically and metabolically improbable due to the energetic costs but not out of the question; there are numerous marine species,[19] including bivalves[20] related to the common blue mussel, and sabellid tubeworms[21] related to sandcastle worms that chemically bore tubes into calcium carbonate rocks with acidic secretions. Although it is apparently biologically possible, to our knowledge, no evidence has been reported that mussels, barnacles, or sandcastle worms prepare surfaces for bonding by acid treatment. The second scenario seems more likely given the ubiquity of fouled surfaces in natural aquatic environments and that aquatic animals evolved in their midst. Natural underwater adhesion to low-energy native surfaces may be fundamentally a process of ion and ligand exchange; the sidechains of adhesive proteins displace surface adsorbed water, ions, and weakly bound polyions that are ubiquitous in natural water.

Surface Charge and Electrical Double Layer of (Hydr)oxide Surface

Aquatic organisms can adhere to natural organic substrates as evident by the presence of barnacles on the bottoms of wooden boats and the backs of whales. In the laboratory, aquatic organisms will adhere to substrates not commonly found in nature, such as Teflon (polytetrafluoroethylene), paraffin wax,[14,22,23] self-assembled monolayers with surface energies designed from high to low,[24,25] and fouling-release polydimethyl siloxanes.[26] In laboratory experiments, marine organisms given a choice of substrate seemed to prefer higher energy hydrophilic surfaces over lower energy hydrophobic surfaces.[27,28] The bond strengths, in the few cases they were estimated, were lower on low energy surfaces.[14,26] For the most part, though, aquatic organisms in nature adhere to, or join together "rocks," which are comprised of one or more minerals. It is therefore appropriate to focus on mechanisms of adhesion to common minerals in the environment.

The most common rock-forming minerals encountered by aquatic organisms are silicates—silicon oxides ($[SiO_4]^{4-}$, $[Si_2O_7]^{6-}$, or Si_2O_5) joined by interstitial metal cations, predominantly Al, Mg, Ca, and Fe—and metal oxides, predominantly of Al and Fe. Carbonate minerals, geologic and biogenic, are also common in the marine environment. In natural waters, pristine oxide minerals rapidly acquire surface charge through several mechanisms. The metal ions in the surface layer have a reduced number of coordination bonds compared with those in the interior and hence behave as Lewis acids capable of coordinating with Lewis bases. In pure water, most are hydroxylated by the dissociative coordination of water molecules.[27] The resulting metal hydroxides are amphoteric with pH-dependent surface charge: positive at low pH, negative at high pH (Fig. 2). Silanol groups on the surface of silica are likewise amphoteric. As a consequence of the surface acid-base chemistry, there is a characteristic pH value, referred to the pristine point of zero charge (PPZC), at which the net charge of the mineral surface is neutral. Depending on pH, a (hydr)oxide surface can therefore interact with both Lewis acids and bases, or anions and cations. Surface charges can also arise at lattice imperfections due to isomorphous replacement of constituent metal ions with metal ions of different charge. By any mechanism, surface charge results in the formation of an electric double layer—enrichment near the surface of ions with charge

Acid-base equilibria:

1) $\equiv S{-}OH_2^+ \leftrightarrow \equiv S{-}OH + H^+ \leftrightarrow \equiv S{-}O^- + 2H^+$

Metal binding:

2) $\equiv S{-}OH + M^{z+} \leftrightarrow \equiv S{-}OM^{(z-1)+} + H^+$

3) $\begin{matrix}\equiv S{-}OH \\ \vdots \\ \equiv S{-}OH\end{matrix} + M^{z+} \leftrightarrow \begin{matrix}\equiv S{-}O \\ \vdots \\ \equiv S{-}O\end{matrix}\!\!\diagdown\!\!\diagup M^{(z-2)+} + 2H^+$

Ligand exchange:

4) $\equiv S{-}OH + L^- \leftrightarrow \equiv S{-}L + OH^-$

5) $\begin{matrix}\equiv S{-}OH \\ \vdots \\ \equiv S{-}OH\end{matrix} + L^- \leftrightarrow \begin{matrix}\equiv S \\ \vdots \\ \equiv S\end{matrix}\!\!\diagdown\!\!\diagup L^+ + 2OH^-$

6) $\begin{matrix}\equiv S{-}L_1 \\ \vdots \\ \equiv S{-}L_1\end{matrix} + L_2^- \leftrightarrow \begin{matrix}\equiv S \\ \vdots \\ \equiv S\end{matrix}\!\!\diagdown\!\!\diagup L_2^+ + 2L_1^-$

Ternary complex formation:

7) $\equiv S{-}OH + L^- + M^{z+} \leftrightarrow \equiv S{-}L{-}M^{z+} + OH^-$

8) $\equiv S{-}OH + L^- + M^{z+} \leftrightarrow \equiv S{-}OM{-}L^{(z-2)+} + H^+$

FIGURE 2 A variety of interactions will determine the chemical species at the mineral solution interface. Metal (hydr)oxide surfaces have pH-dependent charge and a characteristic point of zero charge (PPZC). Such surfaces can interact with either Lewis acids and bases, or anions and cations. Metal ions and other ligands can bind directly to the surface groups through ionic and coordinative bonds, or indirectly through ternary complex formation. Bound ligands can be displaced by ligands with higher affinity for the surface site. S = surface, M^z = metal ion, and L = ligand.

opposite to the surface charge and depletion of ions with the same charge, establishing and maintaining overall electrical neutrality of the ion cloud (Fig. 3). Generally, the formation of the electric double layer is due to the balance of electrical attraction and repulsion and entropy, which tends to scatter ions evenly throughout the liquid phase.

In natural waters that contain numerous dissolved ions, inorganic and organic, interfacial equilibrium is not established by the simple creation of the electric double layer; numerous other "specific adsorption" reactions occur in which the interactions between dissolved ions and the surface are predominantly chemical rather than coulombic. Ions that form specific coordination complexes in solution are capable of forming similar complexes with the same chemical groups on metal (hydr)oxide surfaces.[28] This is illustrated by the general trend of the measured surface complex equilibrium constant to be similar in magnitude to the solution complex equilibrium constant for a series of acids (Fig. 4). Monobasic phosphate is a notable outlier; it tends to form more stable surface complexes than solution complexes with α-FeOOH (goethite).

Several mechanisms of complex formation on a mineral hydroxide surface are diagrammed in Figure 2. (1) Acid–base chemistry of surface hydroxyls creates pH-dependent charge. (2) Protons are Lewis acids readily displaced by stronger Lewis acid metal ions. (3) Multivalent metal ions can from bidentate coordination complexes with the surface. (4) Anionic ligands can displace surface hydroxides and water to form coordination bonds with surface metal ions, or (5)

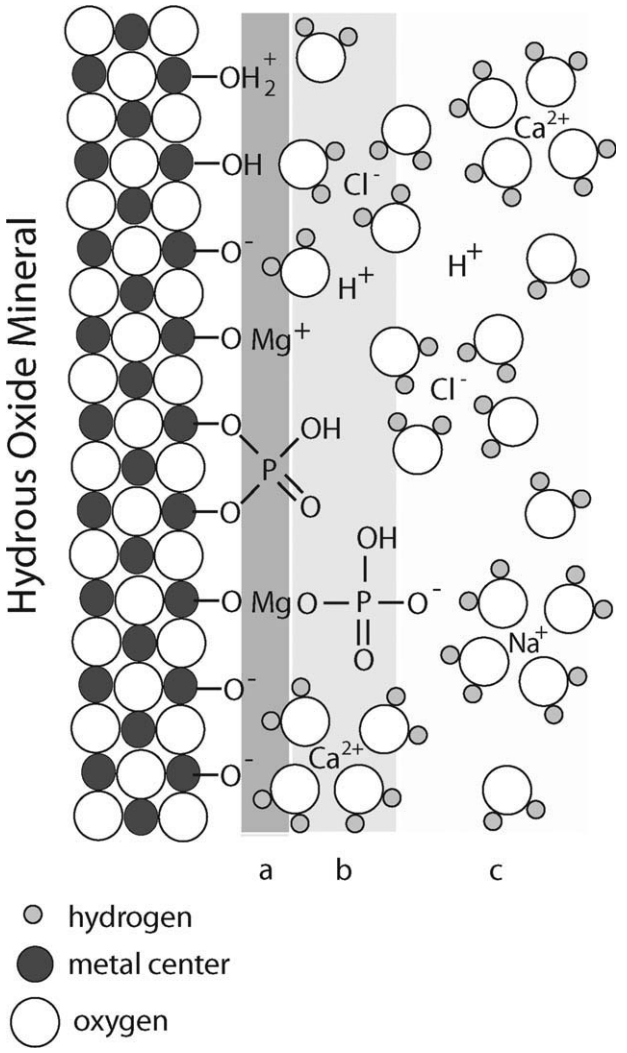

FIGURE 3 At equilibrium, some ions may be adsorbed as inner sphere complexes (layer a), outer sphere complexes where the ions are separated from surface ions by one or more water molecule layers (layer b), a diffuse layer of ions where thermal motion begins to overcome the exponentially decaying electrostatic forces (layer c).

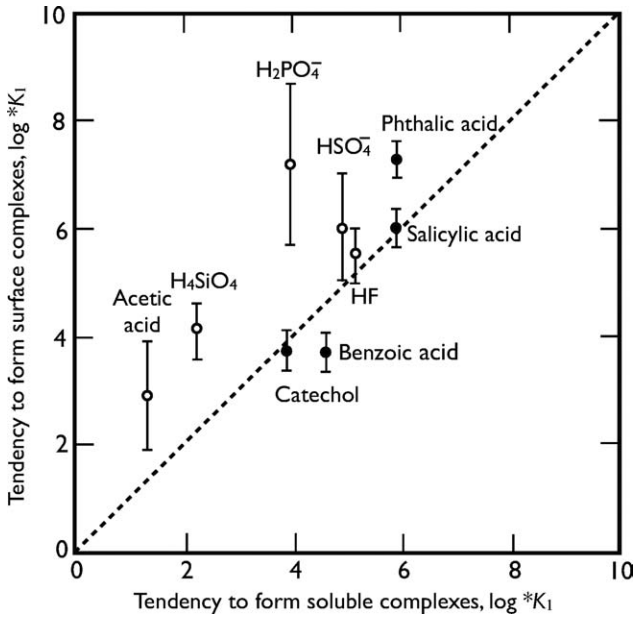

FIGURE 4 Relationship between complex formation in solution and at metal oxide surfaces. Ligands that form stable complexes in solution will form similarly stable complexes with the same groups at a surface. Open symbols: α-FeOOH, closed symbols: γ-Al_2O_3. Reproduced with permission from Croatica Chemica Acta.[28]

bidentate surface complexes. These are inner sphere coordination bonds, largely covalent in nature. As cited later, these complexes can form even on the "wrong side" of the surface PPZC, that is, where adsorption of an ion occurs against repulsive coulombic forces. (6) Specific adsorption is a dynamic process; the distribution of competing ligands, L_2 and L_1, on the surface site, S, is determined by their relative affinities and concentrations. (7) Metal ions can be adsorbed through a ternary complex with an intermediary ligand, or (8) vice versa.

Natural adhesion to low energy native surfaces is likely dominated by the displacement of surface bound ion and ligands by the sidechains of adhesive proteins. The driving force for ligand exchange reactions is a decrease in free energy:

$$\Delta G_{ex} = RT \ln K_{ex} = \Delta H_{ex} - T\Delta S_{ex}$$

where ΔH_{ex} and ΔS_{ex} are the enthalpy and entropy of the exchange process and K_{ex} is the exchange equilibrium constant defined, for scheme 6, as:

$$K_{ex} = \frac{\{\equiv S - L_2^+ - S \equiv\}[L_1^-]_0^2}{\{\equiv S - L_1\}^2[L_2^-]_0} = \frac{\{\equiv S - L_2^+ - S \equiv\}[L_1^-]_b^2 e^{2zF\varphi_0/RT}}{\{\equiv S - L_1\}^2[L_2^-]_b e^{zF\varphi_0/Rt}}.$$

where { } denotes the surface concentration (mol/m^2), and [ ]$_0$ denotes the solution ligand concentration (mol/L) in the immediate vicinity of the surface, where the electrical potential is ϕ_0. The concentration of the ligands next to the surface is related to the bulk solution ligand concentration by Boltzmann's law, hence, the exponential terms where zF is the ligand charge in Coulombs. In the parlance of ion exchange chromatography, the exchange equilibrium constant is referred to as a "selectivity coefficient," defined as the ratio of the ligand affinities for the surface site.[29]

The change in free energy depends on the chemical nature of the surface binding site, the competing ligands, and the hydration shell around them. Ions influence the structure of water differently with important consequences; so-called kosmotropes[30] order water, while chaotropes disrupt water structure.[31,32] In general, small ions attract water dipoles more strongly than larger ions of the same charge, thus, creating a more oriented hydration shell than larger ions. The Jones-Dole viscosity B coefficients (Table 1) are a direct measure of an ion's kosmotropy ($B > 0$) or chaotropy ($B < 0$) and are linearly related to $-\Delta S_{solvation}$.[33] Hence, hydration entropy is negative for small ions and positive for large ions. The sign of the ionic charge is critical as well. Comparing F^- and K^+, ions with similar radii, the hydration entropy of the anion is negative, and of the cation positive. Large or weakly charged ions are surrounded by a hydrogen-bonded water cage and, when paired with another large ion of opposite charge, often form insoluble salt due to hydrophobic-like attractions.[33] Similar effects are expected in the surface binding site–ligand interactions: the low solubility of large ion salts translates to a stronger ligand binding to the surface site if the appropriate pairing is available. The entropic contribution to the free energy of ligand exchange depends on the difference between the ways in which the water molecules are patterned around the ligands. The release of highly ordered, or H-bonded water molecules around the ligand will increase the entropy of the system. Phosphate, for example, ranks high on the viscosity B coefficients list (Table 1); its affinity for a solid–liquid interface, whether as a small ion or as part of a macromolecule, is in part driven by the release of a highly ordered shell of water.

TABLE 1 Jones-Dole Viscosity B Coefficients

	Cations	B	Anions	B
Kosmotropes	Mg^{2+}	0.385	PO_4^{3-}	0.590
	Ca^{2+}	0.285	CH_3COO^-	0.250
	Ba^{2+}	0.22	SO_4^{2-}	0.208
	Li^+	0.150	F^-	0.1
	Na^+	0.086	$HCOO^-$	0.052
Chaotropes	K^+	−0.007	Cl^-	−0.007
	NH_4^+	−0.007	Br^-	−0.032
	Rb^+	−0.030	NO_3^-	−0.046
	Cs^+	−0.045	ClO_4^-	−0.061
			I^-	−0.068
			SCN^-	−0.103

Adapted from ref. 31.

Polymeric Surface Contaminants

In addition to simple and complex ions, natural waters contain ubiquitous biopolymeric substances, collectively known as humic and fulvic acids, that originate from the decomposition of plant and animal matter. These are complex mixtures of polydisperse compounds with poorly defined structures, ranging in molecular weight from hundreds to tens of thousands, containing carboxyl, hydroxyl, methoxyl, phenolic, catechol, and aliphatic moieties.[34] They are surface active—accumulate at interfaces between phases—through several mechanisms, including electrostatic association, surface complex formation, and hydrophobic interactions.[35,36] The multitude of functional groups also creates abundant opportunity for metal ion complexation and chelation by the surface adsorbed polymers, effectively concentrating metal ions at the interface.[34] Another category of ubiquitous surface-associated biopolymers are produced by sessile microbes. These sometimes elaborately structured, almost tissue-like biofilms are predominantly comprised of anionic exopolysaccharides, but also contain proteins, and extracellular DNA.[37,38] Calcium and magnesium cations are also abundant and are critical for biofilm architecture.

Adhesive Protein Adsorption in Natural Waters

How do the adhesives of aquatic organisms adhere to, or penetrate the ionic and polyelectrolyte clouds near native, low-energy, mineral surfaces? The chemical nature of the amino acid sidechain functional groups and their effective concentrations in the proteins that make contact with the surface probably play a dominant role. In addition to the genetically encoded amino acids (Fig. 5, top row), amino acids with post-translationally modified sidechains (Fig. 5, bottom row) are extensively used (Table 2). The mussel adhesive plaque proteins[49] found at the interface with the substrate are illustrative: mfp-3 contains 20 mol % hydroxylated tyrosine (dopa) and 19 mol % 4-hydroxylated arginine; mfp-5 contains 25 mol % dopa and 10 mol % phosphorylated serine (pSer).[46] The proteins are polybasic. The sandcastle worm also exploits modified sidechains. On the whole, the glue contains 2–3 mol % unoxidized dopa and ~30 mol % pSer.[50–52] The phosphoserines occur in the Pc-3 set of proteins, at up to 80 mol %, in runs of 4–13 residues separated by single tyrosine residues, which may be hydroxylated to form dopa. The sandcastle glue also contains at least three dopa-rich, basic proteins, Pc-1, -2, and -5. It is not known whether any of the proteins are strictly interfacial. Similarly, the sticky underwater silk of aquatic caddisflies, on the whole, contains 10 mol % pSer, which occur in the silk heavy chain protein (H-fibroin) as repeating blocks of $(pSerX)_4$. The H-fibroins also contain ~15 mol % basic residues, mostly arginine that occur in blocks that alternate with the pSer blocks.[48] The cement proteins of acorn barnacles are exceptional in that they have been reported to be unmodified post-translationally, but unexceptional in having a preponderance of polar residues.[47,53] The proposed surface primers, Cp19k and Cp20k, have nearly balanced acidic and basic residues and have slightly acidic isoelectric points (Table 2).

Of the several amino acid functionalities at the adhesive interface, the catechol sidechain of L-dopa has received, far and away, the most publicity as a biomimetic adhesion promoter.[54–58] The adsorption mechanism of catechols and catechol derivatives on metal oxide surfaces has been well studied. Comparisons of infrared (IR) spectra of catechol complexes in solution with spectra of catechols adsorbed to thin metal oxide surface layers revealed that catechols adsorb by ligand exchange of coordinated water and hydroxyl ions to form bidentate inner sphere complexes.[59,60] As such, they are logical underwater adhesion promoters.[61] Other adsorption studies established that the *ortho*-dihydroxy configuration is necessary for strong absorption; *meta*- or *para*-dihydroxybenzenes do not adsorb appreciably, nor does L-tyrosine or L-phenylalanine.[62,63]

The adsorption of L-dopa onto TiO_2 surfaces has also been measured mechanically by atomic force microscopy (AFM).[64] Polyethylene glycol-passivated AFM tips, modified with a low density of L-dopa, repeatedly brought into contact with a thin TiO_2 layer on a silicon surface, then retracted, displayed consistent elastic extension events followed by abrupt detachments. The mean detachment force at neutral pH from dozens of events with the same tip and presumably the same single L-dopa molecule was 805 $\pm$ 131 pN at a 60 nN/s loading rate. Mechanical measurements of catechol adhesion to TiO_2 have also been made using a reversed experimental set-up.[65] A series of dopamine methacrylamide-*co*-butylamine methacrylamide copolymers, with sidechain concentrations ranging inversely from 0–100 mol %, were adsorbed at low density onto a TiO_2 substrate and probed with a TiO_2-coated AFM tip. After an initial contact adhesion force was overcome, a constant force plateau was observed on further retraction of the AFM tip from the copolymer-coated surface. The force profiles were interpreted as a saw tooth pattern (hidden in the thermal noise) arising from the peeling off of a single copolymer, sequentially resisted by individual catechol surface bonds. The mean adhesion force at the plateau, 67 $\pm$ 11 pN, an order of magnitude lower than the earlier measurements, was independent (except for 0 mol %) of the catechol sidechain concentration.

Phosphate is not generally thought of as a biomimetic adhesion promoter, though it is becoming increasingly apparent that phosphoserines are more common in underwater bioadhesives, freshwater, and marine, than dopa. In addition to mussels,[66] sandcastle worms,[52] and caddisfly silk,[48] peptidyl phosphate also occurs in the sticky defensive secretion of sea cucumbers,[66] and kelp spore adhesive.[6] The strong and water-resistant adsorption of phosphates (and phosphonates) to surfaces has long been appreciated in several industries: water-borne latex paints contain polyphosphates to promote wet adhesion and scrub resistance,[67] dental materials contain phosphates to adhere to dentin and enamel,[68,69] and phosphates are widely used to inhibit corrosion of iron, steel, and aluminum.[70] Surface modification of metal oxides with alkyl phosph(on)ates has been extensively investigated[71] as a means of forming self-assembling

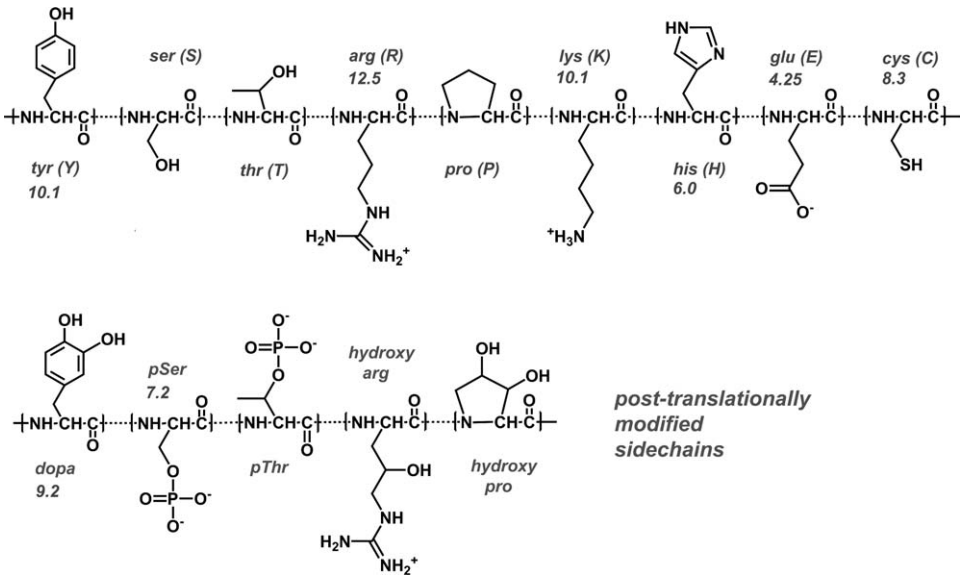

FIGURE 5 Amino acid sidechains. Top row: standard genetically encoded amino acids. Bottom row: post-translationally modified amino acids found in natural underwater adhesives. The numbers below the three-letter code are the sidechain pK_a values for the free amino acids[39] and pK_{a2} for the phosphoserine. The pK_a values can vary dramatically due to the local environment.

TABLE 2 Amino Acid Composition of Adhesive Proteins

	Mussels					Sandcastle Worms					Barnacles					Caddis Larvae
Protein	mfp-1	mfp-2	mfp-3	mfp-4	mfp-5	Pc-1	Pc-2	Pc-3x	Pc-4	Pc-5	cp-19k	cp-20k	cp-52k	cp-68k	cp-100k	Silk
pI ⇒	10.0	9.2	10.4	10.2	9.8	9.7	9.9	–	9.5	10.3	5.9	4.8	unk	unk	9.6	n/a
Gly	0.4	13.6	25.0	5.2	20.3	45.5	28.2	0.0	33.7	22.5	15.5	5.5	16.5	14.8	4.2	20.1
Ala	6.1	2.7	2.1	4.5	4.1	6.7	19.5	0.0	7.7	10.1	10.3	4.4	13.5	12.4	5.6	6.3
Thr	13.0	4.1	0.0	2.8	0.0	0.0	1.5	0.0	2.8	1.6	12.1	3.8	12.9	13.8	4.6	3.2
Ile	1.5	0.8	0.0	4.3	0.0	1.1	0.5	0.0	1.6	3.1	2.9	1.6	2.6	1.7	7.7	3.8
Leu	1.3	1.2	0.0	6.8	0.0	2.8	3.1	0.0	7.7	6.2	5.7	1.6	3.2	1.8	11.4	6.0
Val	1.0	4.1	0.0	12.6	0.0	6.2	6.2	0.0	7.7	6.2	8.0	2.7	6.2	7.3	7.1	4.1
Tyr	*19.1*	*7.6*	*20.8*	*2.3*	*27.0*	*18.5*	*9.2*	*10.7*	*10.6*	*4.7*	0.0	3.3	0.4	0.5	6.3	4.1
dopa	**13**	**3-5**	**20**	**1-2**	**26**	**9.8**	**7.3**	**?**	**?**	**?**	–	–	–	–	–	–
Cys	0.2	14.6	0.0	0.3	0.0	3.4	1.5	0.6	0.8	0.0	1.1	17.6	0.7	0.9	1.4	–
Phe	0.0	1.0	0.0	1.3	0.0	0.0	1.5	0.0	0.0	3.1	2.3	0.5	1.4	0.7	4.7	1.2
Pro	24.8	10.1	6.2	0.7	1.4	0.0	3.6	0.0	2.4	12.4	2.9	6.0	5.1	2.5	4.9	4.0
hPro	**20**	–	–	–	–	–	–	–	–	–	–	–	–	–	–	–
Ser	9.2	6.0	0.0	4.5	**10.8**	0.6	3.6	88.1	3.3	1.6	10.3	6.6	12.8	16.0	8.6	15.4
pSer	–	–	–	–	**10**	–	–	**84**	–	–	–	–	–	–	–	**10**
Asp	0.2	3.9	2.1	5.1	0.0	0.0	0.0	0.0	0.0	0.0	5.7	11.5	6.6	8.8	3.7	11.7
Glu	0.2	2.3	0.0	2.4	2.7	0.0	0.0	0.0	0.0	0.0	5.2	10.4	9.7	8.7	4.0	3.5
Arg	0.2	5.3	18.8	7.1	2.7	0.6	2.1	0.3	0.4	3.1	0.6	2.2	3.0	3.6	6.9	8.8
hArg	–	–	**19**	–	–	–	–	–	–	–	–	–	–	–	–	–
His	0.0	0.6	0.0	23.6	6.8	0.0	8.7	0.0	12.6	12.4	0.6	9.9	0.3	.25	1.3	0.7
Lys	21.2	12.1	4.2	5.5	20.3	14.0	6.7	0.3	4.1	2.3	9.8	5.5	4.8	5.1	5.5	4.2

Acidic residues are shaded blue, basic residues red. Compositions were derived from the following sources: mfp-1 [96, 143], mfp-2 [1][93], mfp-3 [144, 145], mfp-4 [146], mfp-5 [37], Pc1-5, Cp-19k, Cp-20k, Cp-100k from DNA sequences deposited in Genbank, Cp-52k and Cp-68k [42], and Caddisfly larval silk [41]. The mol % modified residues is shown under the mol % unmodified residues determined from DNA sequences.

monolayers with high hydrolytic stability.[73,73] Nonfouling surfaces have been created by anchoring polyethylene glycol (PEG) to TiO_2 surfaces through poly(alkyl phosphonate).[74] Glycans modified with alkyl phosphonate tails were arrayed on AlO_2-coated glass slides by a simple spotting procedure for high-throughput screening of protein carbohydrate interactions.[75]

Environmental scientists interested in the disposition of phosphorus fertilizers in the environment have created a ripe literature on the adsorption mechanisms of phosphates onto metal oxide minerals. As revealed primarily by surface sensitive IR spectroscopy techniques, phosphates, at subsaturating concentrations, adsorb onto metal (hydr)oxide surfaces as inner-sphere, bidentate complexes (Fig. 3) over a broad pH range.[76–79] In the pH range 4.0–7.5, phosphate adsorption onto goethite particles (FeO(OH)) was independent of ionic strength up to 0.8 M NaCl, the highest concentration tested. Above pH 7.5, phosphate adsorption increased with increasing ionic strength.[80] Above the point of zero charge (pH 9.2), where goethite has a negative surface charge, phosphate adsorbed against repulsive coulombic forces. High salt concentrations may shield the repulsive electrostatic forces.[81] The ionic strength and surface charge independence is further evidence the predominant phosphate complex is more coordinative in nature than electrostatic, observations that are of particular relevance for peptidyl phosphates as adhesion promoters in marine bioadhesives.

Competitive adsorption studies of phosphate with several chemically distinct compounds further illustrate why phosphates may be a common adhesion promoter in natural adhesives. Phosphate competed effectively with equal concentrations of catechol for adsorption onto aluminum (hydr)oxide, suppressing catechol adsorption from 25–50% depending on the mineral crystal form, suggesting similar affinities.[59] It follows that a polyphosphate, with a high local effective concentration of phosphate groups, may be able to displace even a bacterial biofilm surface anchored through catechol containing siderophores.[82] Sulfate adsorption to goethite is ionic strength dependent, demonstrating the predominantly electrostatic character. Sulfate competes poorly with phosphate below pH 6 and does not compete at elevated pH as the surface becomes more negatively charged.[83] The implication is that a phosphorylated protein may readily displace surface-bound sulfated exopolysaccharides, seaweed-derived carrageenans for example. Citrate, a tricarboxylic acid, likewise competes weakly with phosphate for adsorption to goethite below pH 7.[84] Exopolysaccharides with carboxylate groups may be displaced by phosphoproteins.

The high concentrations of basic amino acids, positively charged at neutral pH, suggest an important role in adhesion. The imidazole sidechain of histidine is the most chemically versatile of the basic residues. With nominal pK_a 6–7, the sidechain can change from being positively charged to uncharged within a pH range spanning neutral pH.[85] A second significant character of histidines is their ability to form metal coordination complexes at pH above the sidechain pK_a,[86] as attested by the well-known practice of attaching histidine peptide tags to recombinant proteins to facilitate purification on immobilized metal ions, such as Ni(II) chelated to nitrilotriacetic acid groups.[87] The enthalpies of metal complexes of Co, Ni, Cu, and Zn with L-histidine ($M(II)(His^-)^2$) are between −10 and −22 kcal/mol.[86] Similar histidine-metal ion coordination complexes would also form when the metal ions are liganded to the surfaces of clays, zeolites, and silica[88–90] or are complexed with surface-adsorbed humic acids.

The adsorption of lysine and arginine onto oxide particle surfaces and biopolymer surface films, most of which are negatively charged at neutral pH values, appears to be primarily electrostatic. Adsorption of free lysine adsorbed from neutral pH solution onto a clay silicate (montmorillonite) and TiO_2 is driven primarily by electrostatic interactions based on the similarity of IR spectra of free and adsorbed lysine[92,93] with a binding free energy of several kJ/mol.[93,94] Arginine interactions with apatitic phosphates are largely mediated by electrostatic interactions through the positive charge on the guanido sidechain (pK_a 12.5) as well as H-bonding.[95,96]

Synergistic Polymer Effects

The individual functional sidechains of the interfacial adhesive proteins adsorb to charged native metal (hydr)oxide surfaces by the generic ligand (ion) exchange mechanisms (Fig. 2) and thermodynamic considerations discussed previously. The variety and potential combinations of functional groups with mixed adsorption mechanisms allows aquatic organisms to attach to native surfaces with likewise varied and mixed characteristics, an obvious selective advantage. The overall surface affinity of the proteins is amplified by the multiplicity of the interactions, a synergistic "zippering" effect, described earlier for mussel adhesion,[2] where adsorption of the first ligand increases the association constants for subsequent ligand adsorption. The result is robust adsorption and a low probability of spontaneous desorption even for weakly adsorbed individual ligands. A monovalent ligand dissociates from its binding site with probability

$$p_{\mathrm{mono}} = \frac{k_{\mathrm{off}}}{k_{\mathrm{on}}[L] + k_{\mathrm{off}}},$$

where $[L]$ is the concentration of ligands, k_{off} and k_{on} are the dissociation and association rate constants, respectively. When N individual ligands are linked through a protein backbone the probability of simultaneous dissociation of N ligands is

$$p_{\mathrm{ploy}} = \left(\frac{k_{\mathrm{off}}}{k_{\mathrm{on}}[L] + k_{\mathrm{off}}}\right)^N.$$

Nonetheless, macromolecule adsorption is dynamic and reversible; bound macromolecules can be "eluted" by changes in pH, salt concentration, or by ions with a high selectivity coefficient than the adsorbed ion. This is obvious in the practice of protein ion exchange chromatography. Likewise, surface-bound macromolecules can be partially or completely

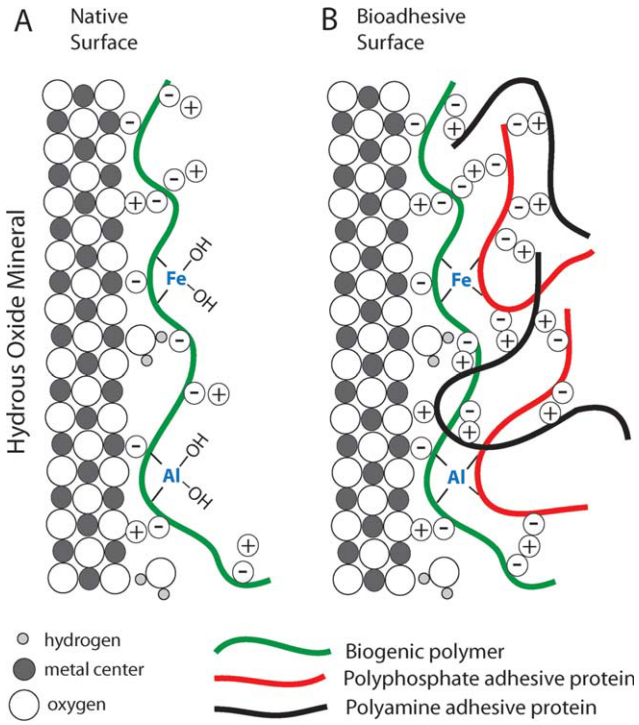

FIGURE 6 Adhesive protein adsorption to native surfaces. (A) Biogenic surface-adsorbed polymers, such as humic and fulvic acids, may serve as preprimers for natural underwater adhesives. The polymers are known to complex metal ions and concentrate them near the surface. (B) Adhesive proteins can adsorb to the priming polymer layer through a combination of electrostatic interactions, ternary metal complex formation, or though diffusive interpenetration and physical entanglement of polymer chains. Histidine, phosphoserine, and dopa residues are all capable of forming ternary coordination complexes with immobilized metal ions. In the absence of polymeric surface contaminants underwater adhesives can directly adsorb to surfaces through similar mechanisms.

displaced by other macromolecules with higher chemical affinity and/or effective concentration of complex forming functional groups. Hence, adhesive proteins may be able to displace relatively weakly bound humic acids from native surfaces during adsorption. Alternatively, or in addition, tightly bound humic polyions may be exploited by aquatic organisms as preprimers, or conditioning films [Fig. 6(A)] onto which adhesive proteins adsorb directly through a combination of electrostatic interactions, ternary metal complex formation [Fig. 6(B)], or though diffusive interpenetration and physical entanglement of polymer chains [Fig. 6(B)]. Histidines, phosphoserines, and dopa residues are all capable of forming ternary metal coordination complexes. Significantly, as much as 80% of the orthophosphate found in natural water is associated with humic acid as Al(III) or Fe(III) complexes.[97] Polyphosphates in an adhesive protein could associate with surface-bound humic acid through similar metal complexes [Fig. 6(B)]. In contrast to electrostatic interactions, such complexes are insensitive to the high dielectric constant of water and to the presence of salts in marine environments.

Surface adsorption of polyelectrolytes from dilute solutions has been well-studied by practitioners of the layer-by-layer approach to forming surface films.[98] The surface adsorption of a polyelectrolyte from dilute solution is opposed by the reduction of the polymer's configurational entropy; in bulk solution, the polymer can explore a nearly infinite set of configurations, a set which is greatly reduced when the polymer is fixed at the interface. The loss of entropy by the polyelectrolyte is more than compensated by the gain in entropy of the displaced surface-bound water and microions, resulting in a net thermodynamic driving force for polyelectrolyte adsorption.[99,100] In comparison, underwater adhesive proteins adsorb from highly concentrated solutions, perhaps complexed with other proteins.[52] An important implication is that the entropic penalty for surface immobilization may be lower, because the proteins are already in a restricted configurational space. As a result, the net gain in entropy for adsorption of concentrated, precomplexed proteins may be larger than single polyelectrolyte adsorption from dilute solution.

Role of Protein (Polymer) Structure in Interfacial Adhesion

Few experiments have been reported that systematically investigate the role of adhesive protein sequence or higher order structure in interfacial adhesion. A linear polyethylene glycol (PEG) surface anchored with a single decapeptide repeat from the byssal cuticle protein (mfp-1) was compared with PEG surface anchored with a single dopa residue. Both effectively prevented adhesion of cells to Au and Ti surfaces, demonstrating surface adsorption of PEG, though the decapeptide-terminated PEG was slightly more effective in preventing cell attachment in the indirect assay.[54] (Mfp-1 is a coating on the byssal plaque assembly, hence, the repeating decapeptide plays no role in interfacial adhesion in the natural process and its specific sequence would not be expected to be of particular significance.).

Native surfaces have a variety of chemical features in unpredictable patterns. The optimal sequence and structural solution for adhering to these mixed surfaces would be a mixture of proteins with a variety of adhesion-promoting sidechains in random order and sufficient configurational flexibility to allow functional groups to match up with the mixed surface features. In other words, a mixture of random copolymers. To a very limited extent, this seems to be a strategy used by mussels; a dozen variants of one of the interfacial proteins (mfp-3) were identified that varied in isoelectric point and the numbers of dopa and 4-hydroxyarginine residues.[61] The strategy is limited in natural adhesives, because proteins are made by templated polymerization; aquatic organisms do not have the option of random copolymerization.

GLUE SOLIDIFICATION: COHESION

Natural adhesives, by necessity, are excreted or secreted onto the surface of the adherends as flowable, viscous fluids or colloidal suspensions. After application, the glue must

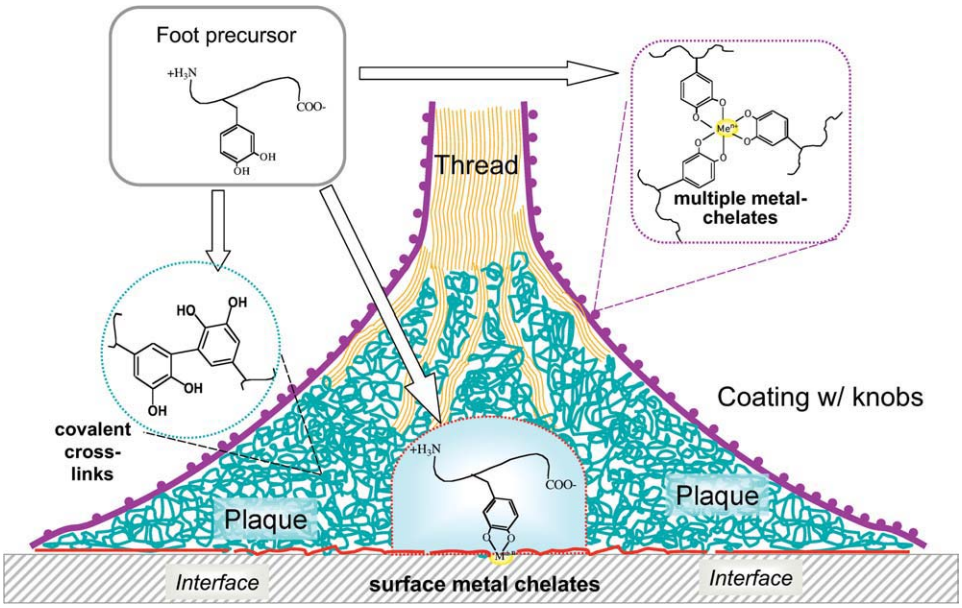

FIGURE 7 The multiple roles of dopa in the mussel adhesive plaque. The protein components are secreted in a temporally and spatially organized sequence. The catechol sidechain of dopa plays an adhesive role through surface coordination complexes and indispensable cohesive roles though Fe(III) complex formation and oxidative covalent crosslinking through quinone intermediates. Adapted by H. Waite from ref. 101.

quickly solidify to form a load-bearing joint. Mussels are tethered to wet surfaces by a beard of byssal threads. The distal end of each byssus splays into the foamy interior of the plaque—an assemblage of at least six different mussel adhesive plaque proteins organized into a sophisticated thread-to-rock connector (Fig. 7). The plaque proteins are secreted from distinct areas of the foot in a temporally organized sequence; first, the surface coupling proteins (mfp-3, -5); then, the core proteins (mfp-2, -4); and finally, a cuticle, a hard and protective coating (mfp-1), is applied to the entire thread and plaque structure.[102] The sequential assembly of the mussel plaque is superficially reminiscent of a layer-by-layer approach to surface modification. A new weight-bearing thread and plaque assembly can be formed in as little as a minute suggesting rapid and accurately timed solidification of the construct. How are the various components connected into a cohesive assembly?

Part of the answer is through Fe(III)-L-dopa coordination complexes. A potential cohesive role for Fe(III)-L-dopa complexes in the mussel byssus was established some time ago.[103,104] Now, precision experiments with Israelachvili's surface forces apparatus (SFA) with isolated mussel adhesive proteins are resolving the contribution of L-dopa-Fe(III) complexes to the cohesive integrity of the plaque and cuticle. Mica surfaces coated with the most abundant (25 wt %) adhesive plaque protein (mfp-2), which occurs in the plaque core, did not cohere unless low concentrations of Fe^{3+} and/or Ca^{2+} were added. Fe^{3+} increased cohesion five to seven times more than Ca^{2+}.[42] Though mfp-2 has a comparatively low dopa content (3–5 mol %), the results suggest that L-dopa-Fe(III) complexes play a role in the cohesive integrity of the plaque core.[105] In general, little is known about the higher order structure of natural adhesive proteins. Mfp-2 is one of the few adhesive proteins with a predicted structure, not from experiment, but from sequence homology—it is comprised of 11 consecutive epidermal growth factor (EGF)-like domains. The fold of each roughly 4 kDa domain is stabilized by intermolecular disulfide bonds and one to three dopa residues. The structural effect, perhaps, is to present an organized array of dopa residues, which may guide efficient and accurate assembly of mfp-2 in the plaque core. In this case, higher order structure must be critical to mfp-2 function or the sequences of the individual EFG-like repeats would have diverged much more than they have. Amino acids with carboxylic acid sidechains (D and E) that can participate in Ca^{2+} bridging are scattered through out the mfp-2 sequence and clustered at both termini.

The cuticle of intertidal mussels, a plum pudding of hard submicrometer granules within a soft extensible matrix, contains a single protein component, mfp-1.[106] Purified mfp-1 was lousy glue that did not stick two mica surfaces together.[107] But in the presence of low concentrations of $FeCl_3$, the mfp-1 coated surfaces stuck strongly, evidence of Fe(III)-mediated crosslinking.[40] Another set of experiments using *in situ* resonance Raman spectroscopy demonstrated that tris-dopa-Fe(III) complexes were concentrated within the harder granules relative to the softer matrix.[106] Viewed together, the results created a coherent thesis in which the integrity and modulated mechanical properties of the cuticle are due to the density and clustered distribution of tris-dopa-Fe(III) complexes.

The other cohesive contribution of L-dopa within the byssal plaque assembly is covalent crosslinking (Fig. 7). The two-

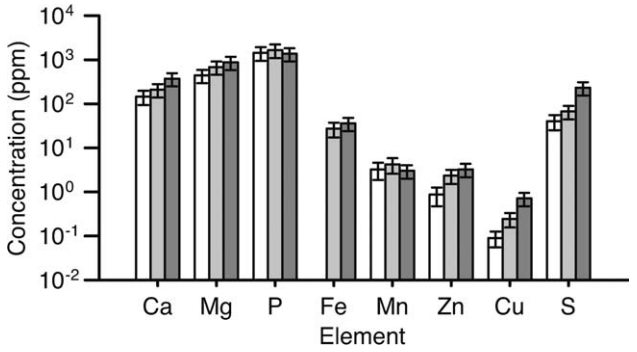

FIGURE 8 Elemental analysis of sandcastle glue. Sandcastle worms rebuilt portions of their tubes in the lab with 0.5 mM beads of various composition: silica (white columns), FSZ (light gray), and YSZ (dark gray). The glued beads were collected and washed with 10 mM Tris, pH 8.2 to remove seawater, and lyophilized. Background measurements were made with unglued beads collected from the same tank at the same time. Glue was digested in concentrated nitric acid and analyzed by inductively coupled plasma optical emission spectroscopy (Perkin Elmer Optima 3100 XL ICP-OES). To estimate molar ratios of elements and amino acids, previously published amino acid data[4] was normalized to the measured amount of phosphorus, based on the assumption that all serine residues in the cement are phosphorylated.[52]

electron oxidation of L-dopa creates a dopaquinone intermediate that undergoes additional reactions through several complicated pathways, including reverse dismutation with dopa resulting in di-dopa crosslinks, addition of nucleophilic sidechains (C, H, K), and conjugation into highly fluorescent, reddish brown to black compounds. Similar chemistry occurs throughout biology, ranging from insect cuticle hardening[108,109] to the production of black eumelanin and red pheomelanin pigments in mammals.[110] Possible pathways from L-dopa to covalent crosslinks have been described elsewhere.[111] In support, di-dopa[112] and cysteinyl-dopa[113,114] crosslinks have been empirically observed in mussel byssus. Wilker and co-workers observed a signal from an organic radical in the electron paramagnetic resonance (EPR) spectrum of mussel adhesive plaques that may connect both phenomena—formation of tris-dopa-Fe(III) complexes and covalent dopa crosslinking. The Wilker model suggests a semiquinone radical is formed by the coupled reduction of Fe(III) and one electron oxidation of L-dopa. Subsequent reaction of the semiquinone radical with O_2 forms a second radical that can participate in covalent crosslinking or coupling to an interface.[115,116] The parsimony of the model is appealing: cohesive integrity is achieved quickly through rapid formation of tris-dopa-iron complexes, slower oxidative decay of dopa-Fe(III) in the presence of O_2 forms permanent covalent bonds, and semiquinone radicals capable of homocoupling into di-dopa are formed directly. Further, preorganization of the adhesive plaque proteins through tris-dopa-Fe(III) complexes before dopa crosslinking may spatially direct the permanent solidification process. In comparison, cosecretion of a catechol oxidase enzyme[117] seems more expensive, less efficient, and too slow in the viscous and hardening plaque, where diffusion of an enzyme and its substrate would be highly restricted. A reasonable conclusion from the forgoing observations is that a critical, indispensable role of dopa in the mussel byssus is cohesion, primarily through metal complex formation, secondly by covalent crosslinking.

The sandcastle glue of *Phragmatopoma californica* sets up into a creamy-white, load-bearing, solid foam within 30 s after secretion.[118] The proteinaceous glue contains substantial amounts of phosphorus, as expected from the high phosphoserine content of Pc3, as well as high levels of Mg and Ca.[52] Quantitative elemental analysis demonstrated that the Mg:Ca ratio was 4:1 and (Mg + Ca):phosphorus ranged from 0.5 to 1.0 (Fig. 8). Although reported estimates vary, the pH of secretory granules from numerous cell types are acidic.[119–121] There is no reason to believe that the regulated secretory system of the sandcastle worm is different, and therefore, the contents of the adhesive secretory granules likely experience an abrupt pH transition when secreted into seawater (pH 8.2). As the second dissociation of phosphate (pK_{a2} 7.2) occurs between these pH values, Pc3 would acquire a substantially higher negative charge in seawater. Insolubilization of Pc3 and divalent cations as a result of the pH transition was proposed as the mechanism driving the initial rapid solidification reaction.[52] Water freed by the dehydration of the glue protein could coalesce to form the porous foam structure of the solid glue. The hypothesis was tested empirically with a Pc3 analog methacrylate copolymer with the similar phosphate sidechain density (80 mol %) and same approximate M_n (60 kDa) as fully phosphorylated Pc3.[122] At pH 5.0, the phosphate copolymer was completely soluble at Mg^{2+} to phosphate sidechain ratios as high as 3:1 but insoluble at 1:1 ratios in artificial seawater at pH 8.2. The pH-triggered insolubilization of polyphosphoproteins with divalent cations is a fail-safe timing mechanism, with minimal biochemical "moving parts" that prevents premature solidification of the sandcastle glue within the secretory system, yet ensures rapid solidification after secretion.

As most underwater bioadhesives are products of the regulated secretory pathway, differential solubility between internal and external pH may be a simple and widespread mechanism that drives solidification. The insolubility of purified mussel adhesive proteins, native and recombinant, at and above neutral pH is sometimes mentioned in the context of confounding *in vitro* experiments, which as a consequence have to be done at acid pH.[42,123,124] Perhaps the general insolubility of the mussel adhesive proteins at seawater pH is an additional adaptation that contributes to solidification and byssus cohesive integrity. The pH of the caddisfly larval silk gland has not been measured, to our knowledge, but the lumen of the silk gland of *Bombyx mori* larvae, silkworms, a terrestrial relative of caddisflies, was reported to be in the range of pH 5–6,[125] and the rheological properties of silkworm silk are pH-dependent.[126] The presence of Ca^{2+} and peptidyl phosphate in caddisfly silk suggest a pH change coupled to extrusion into slightly basic water could contribute to insolubilization of the silk fibers.

Sandcastle worm glue turns progressively more reddish brown during the first several hours after secretion, almost certainly due to dopa-mediated covalent crosslinking, becoming tough yet flexible, like shoe leather. Cysteinyl-dopa adducts present in sandcastle glue provide empirical evidence of covalent crosslinking through dopa.[51] Secreted sandcastle glue contains high concentrations of transition metals relative to seawater (Fig. 8). The Fe concentration, for example, was 6–8 $\times$ 10^5 higher in the glue than in natural seawater[127,128] and even higher compared with the artificial seawater used in the lab aquarium. The Fe concentrations were estimated to be 1/5 to 1/10th the dopa concentrations, a stoichiometric range consistent with Fe-dopa complexes. The other transition metal concentrations were 10^3–10^4-fold higher in the glue than natural seawater. The significance of the transition metals in the sandcastle glue is not known, but their presence suggests metal-dopa or metal-phosphate or metal-histidine complexes could contribute to cohesion, as well as accelerate the nonenzymatic, oxidative crosslinking of the glue through dopa, as proposed in the mussel byssus. In many biochemical contexts, the variety of possible reaction pathways in quinone chemistry would be a liability due to the difficulty of controlling the reactions. In the underwater adhesives of mussels and sandcastle worms, on the other hand, maximizing the number of ways in which complexes and crosslinks can form would be advantageous—dopa seems to fit the role well.

Adult acorn barnacles are attached through a layer of glue between the baseplate and substrate only a few microns thick. As barnacles grow during molting cycles, adhesive originating in unicellular cement glands is transported through a radial canal system of ducts to the periphery of the baseplate.[129,130] The low-viscosity adhesive is initially clear but solidifies and becomes insoluble within 6 h.[131] Whether or not the adult adhesive proteins are synthesized in distinct cell types, how and when they are mixed to form the glue, and the trigger to initiate solidification of the liquid glue are unknown.

The structure of the bulk interior of cured adult barnacle glue has the appearance of a gauze-like fabric,[132] in contrast to the internal solid foam structure of mussel plaques[101] and sandcastle glue.[118] Kamino predicted a fibrous, amyloid-like structure based on the hydropathic profile and predicted β-sheet structure of the cp-100k cement protein (Table 2).[47] The amyloid character of rod-like and nanofibrillar structures were later experimentally observed by AFM and amyloid-specific protein stains.[133,134] Amyloid proteins are famously insoluble and, indeed, fully cured barnacle glue withstands harsh denaturing conditions; complete solubilization of the glue required treatment with 0.5 M dithiolthreitol (DTT), a strong disulfide bond reducing agent, 7 M guanidine hydrochloride, a protein denaturant, and incubation at 60°C for an hour.[47] The requirement for a high concentration of DTT implies a significant role in cohesion for disulfide bonds between cysteine residues. Regarding the solidification trigger, marine bioadhesives experience a substantial increase in ionic strength on excretion that could provide a reliable trigger for solidification similar to, or in conjunction with the pH jump. Indeed, a synthetic peptide derived from a repeating unit of the cp20k that was soluble at low ionic strength, self-assembled irreversibly into a meshwork of insoluble fibrils when the ionic strength was raised to that of seawater.[135]

For completeness, we mention an interesting proposal by Dickinson et al.[136] that solidification of barnacle cement is a specialized form of wound healing. The hypothesis is based on the general similarities in the processes of blood clotting and cement solidification, that is, protein aggregation and crosslinking into fibrils, the broad phylogenetic conservation of the blood clotting biochemical machinery, and the identification of epitopes by western blotting and homologous sequences by tandem mass spectrometry to human trypsin and bovine transglutaminase. Vigorous counter arguments to the theory have been put forward.[137]

SYNTHETIC MIMIC ADHESIVES

The objective of using natural underwater glues, whether gathered, farmed, fermented, or synthesized, for technological purpose has been pursued since at least the late 1960s (see Ref. 138 and references therein) with quite modest commercial success.[139] During the last decade, the adhesion promoting catecholic sidechain of dopa was borrowed from mussels to create several variations of synthetic nonfouling surfaces,[54,51,140–143] to oxidatively crosslink PEG into hydrogels for tissue engineering,[111,144] and to form a sticky layer on a structured surface to create a wet/dry, mussel/gecko adhesive.[145] Polystyrene, not ordinarily a component of adhesives, was turned into a respectable glue by incorporating catechol sidechains.[58] pH-dependent formation of tris-catecholate-Fe complexes, thought to be operational during the formation of the byssus cuticle, has been used to crosslink dopa-terminated PEG into soft gels.[146] Continuing mimetic efforts will likely lead to new mussel-inspired materials that incorporate additional features of the elaborately organized mussel adhesive plaque.

The underwater glue of the sandcastle worm also has been a valuable model for the design of synthetic glues. Synthetic polyelectrolyte analogs with the same sidechain chemistries (phosphates, catechols, and amines) and sidechain molar ratios as the natural glue proteins, mixed in similar proportions as the natural glue, including divalent cations, formed complex coacervates that qualitatively mimicked the entire range of natural glue properties—underwater delivery, wet interfacial adhesion, and triggered solidification.[147,148] The synthetic adhesive coacervates are self-organized in water, water-borne yet water-immiscible, denser than water, "wet" wet surfaces, are ejectable through narrow cannulae, are containers for small molecules, are dimensionally stable after crosslinking fully submerged in water, and can be made inexpensively at scale—ideal properties for underwater adhesives, and medical adhesives in particular. Used to fix rat skull bones, the biomimetic adhesive coacervates did not impede new bone growth, were nontoxic, and did not induce persistent inflammation.[149] Further, adhesive complex

coacervates with bond strengths several times the estimated bond strength of the natural adhesive were created by incorporating additional phases, a common practice in engineering structural adhesives.[150] In short, principles of material design gleaned by studying biology have been unshackled from biological material and material processing constraints.

CONCLUSIONS

The underwater adhesives from four genera of aquatic organisms well illustrate the uniquely specialized adaptations as well as common features of adhesion to native wet surfaces. The form and function are distinct in each case; forms range from an organized layered structure, formed in a mold, to excreted glue, to drawn sticky fibers; functions range from permanently fixing themselves to a surface, to gluing or taping together rocks into protective shells. The shared physical and chemical features include: (i) minimal surface preparation of native surfaces already "passivated" by the spontaneous adsorption of ions, organic matter, and biofilms; (ii) the macromolecular components of the adhesive must competitively displace the "contaminating" ions at the interface, or form ternary coordination complexes; (iii) the adhesive proteins are polyampholytes with amino acid compositions strongly skewed toward ionizable (especially amines) and polar sidechains; (iv) the adhesive proteins usually contain post-translationally modified residues, in some cases hydroxylated tyrosine, in many cases phosphorylated serines; (v) coordinative interactions likely dominate electrostatic interactions in importance at the interface; (vi) the adhesives are delivered to the surface as highly concentrated polyelectrolyte solutions and/or colloidal suspensions; (vii) the high-effective concentrations of amino acid sidechains displace low-affinity ligands and create an essentially irreversible polyvalent bond; (viii) surface bound water is not a significant barrier to adhesion by a water-borne adhesive; (ix) excreted adhesives set and/or harden, in some cases in response to a trigger perhaps as simple as a change in the pH, ionic strength, ion composition, or redox potential of the exterior relative to the interior environment.

There is much more to learn about underwater adhesives from aquatic organisms. Further study, branching out from early well-studied models,[48,151,152] may improve designs and broaden the utility of biomimetic adhesives.

ACKNOWLEDGMENTS

Some of the work described in this review was supported by the NIH (EB006463), the ONR (N00014-10-1-0108), and the NSF (DMR 0906014).

REFERENCES AND NOTES

1 Wiggins, G. B.; Currie, D. C. In Trichoptera Families; Merritt, R. W.; Cummins, K. W.; Berg, M. B., Eds.; Kendall/Hunt Publishing Company: Dubuque, Iowa, **2008.**

2 Waite, J. H. *Chemtech* **1987,** *17*, 692–697.

3 Wiegemann, M. *Aquat. Sci*. **2005,** *67*, 166–176.

4 Jensen, R. A.; Morse, D. E. *J. Comp. Physiol. B* **1988,** *158*, 317–324.

5 Kohn, A. J. *Pacific Sci.* **1961,** *XV*, 163–179.

6 Petrone, L.; Easingwood, R.; Barker, M. F.; McQuillan, A. J. *J. R. Soc. Interface* **2011,** *8*, 410–422.

7 Thomas, L. A.; Hermans, C. O. *Biol. Bull.* **1985,** *169*, 675–688.

8 Costerton, J. W. The Biofilm Primer; Springer: Berlin, **2007.**

9 Pocius, A. V. Adhesion and Adhesive Technology: An Introduction, 2nd ed.; Hanser Gardner: Cincinnati, **2002.**

10 Frantzis, P. *J. Mater. Civil Eng*. **2008,** *20*, 635–639.

11 Cloete, W.; Focke, W. *Int. J. Adhes. Adhes.* **2010,** *30*, 208–213.

12 Biopolymers at Interfaces; Marcel Dekker: New York, **1998.**

13 Glue, adhesive, and cement are often used interchangeably. Here, glue is used to describe materials that chemically bond together two substrates, i.e., are cohesive as well as adhesive. Adhesive is used to describe materials that adhere to an interface but may not be cohesive. Cement is avoided.

14 Burkett, J. R.; Wojtas, J. L.; Cloud, J. L.; Wilker, J. J. *J. Adhes.* **2009,** *85*, 601–615.

15 Smith, A.; Callow, J. Biological Adhesives; Springer, Heidelberg, **2006.**

16 Li, D.; Huson, M.; Graham, L. *Arch. Insect Biochem. Physiol.* **2008,** *69*, 85–105.

17 von Byern, J.; Grunwald, I. Biological Adhesive Systems: From Nature to Technical and Medical Application; Springer-Verlag: Vienna, Austria, **2010**.

18 Kendall, K. Molecular Adhesion and Its Applications: The Sticky Universe; Springer: Frankfurt, **2001.**

19 Stearley, R. F.; Ekdale, A. A. Modern Marine Bioerosion by Macroinvertebrates; Palaios: Northern Gulf of California, **1989; p 453–467.**

20 Goreauand, T. F.; Goreau, N. I.; Yonge, C. M. *J. Zool.* **1972,** *166*, 55–60.

21 Knight-Jones, J.; Chughtai, I. *Zool. Scr.* **1988,** *17*, 231–238.

22 Crisp, D.; Walker, G.; Young, G.; Yule, A. *J. Colloid Interface Sci.* **1985,** *104*, 40–50.

23 Wiegemann, M.; Watermann, B. *J. Adhes. Sci. Technol.* **2003,** *17*, 1957–1977.

24 Aldred, N.; Ista, L.; Callow, M.; Callow, J.; Lopez, G.; Clare, A. *J. R. Soc. Interface* **2006,** *3*, 37–43.

25 Callow, J.; Callow, M.; Ista, L.; Lopez, G.; Chaudhury, M. *J. R. Soc. Interface* **2005,** *2*, 319–325.

26 Kavanagh, C. J.; Schultz, M. P.; Swain, G. W.; Stein, J.; Truby, K.; Wood, C. D. *Biofouling* **2001,** *17*, 155–167.

27 Stumm, W.; Morgan, J. J. Aquatic Chemistry: Chemical Equilibria and Rates in Natural Waters, 3rd ed.; John Wiley and Sons: New York, **1996.**

28 Stumm, W.; Kummert, R.; Sigg, L. *Croat. Chem. Acta* **1980,** *53*, 291–312.

29 Fritz, J.; Gjerde, G. Ion Chromatography, 4th ed.; Wiley-VCH Verlag GmbH & Co. KGaA: Weinheim, **2009.**

30 The empirical Hofmeister series ranks the ions in the order of facilitating the solubility of nonpolar solutes.

31 Kunz, W.; Henle, J.; Ninham, B. W. *Curr. Opin. Colloid Interface Sci.* **2004,** *9*, 19–37.

32 Baldwin, R. L. *Biophys. J.* **1996,** *71*, 2056–2063.

33 Collins, K. *Biophys. J.* **1997,** *72*, 65–76.

34 Snoeyink, V. L.; Jenkins, D. Water Chemistry; John Wiley and Sons: New York, **1980.**

35 Vermeer, A.; Koopal, L. *Langmuir* **1998,** *14*, 4210–4216.

36 Vermeer, A.; Van Riemsdijk, W.; Koopal, L. *Langmuir* **1998,** *14*, 2810–2819.

37 Whitchurch, C. B.; Tolker-Nielsen, T.; Ragas, P. C.; Mattick, J. S. *Science* **2002,** *295*, 1487.

38 Böckelmann, U.; Janke, A.; Kuhn, R.; Neu, T.; Wecke, J.; Lawrence, J., Szewzyk, U. *FEMS Microbiol. Lett.* **2006,** *262*, 31–38.

39 Lehninger, A. L. Biochemistry, 2nd ed.; Worth Publishers: New York, **1970.**

40 Zeng, H.; Hwang, D. S.; Israelachvili, J. N.; Waite, J. H. *Proc. Natl. Acad. Sci. USA* **2010,** *107*, 12850–12853.

41 Silverman, H. G.; Roberto, F. F. U.S. Patent, Battelle Energy Alliance, LLC: Idaho Falls, ID, 6,987,170, **2006.**

42 Hwang, D. S.; Zeng, H.; Masic, A.; Harrington, M. J.; Israelachvili, J. N.; Waite, J. H. *J. Biol. Chem.* **2010;** *285*: 25850–25858.

43 Papov, V. V.; Diamond, T. V.; Biemann, K.; Waite, J. H. *J. Biol. Chem.* **1995,** *270*, 20183–20192.

44 Warner, S. C.; Waite, J. H. *Mar. Biol.* **1999,** *134*, 729–734.

45 Zhao, H.; Waite, J. H. *Biochemistry*. **2006,** *45*, 14223–14231.

46 Waite, J. H.; Qin, X. *Biochemistry* **2001,** *40*, 2887–2893.

47 Kamino, K.; Inoue, K.; Maruyama, T.; Takamatsu, N.; Harayama, S.; Shizuri, Y. *J. Biol. Chem.* **2000,** *275*, 27360–27365.

48 Stewart, R. J.; Wang, C. S. *Biomacromolecules* **2010,** *11*, 969–974.

49 The proteins in the mussel adhesive plaque are referred to as mussel foot proteins (mfps) because they are secreted from the foot. The numbers reflective the order in which the proteins were identified.

50 Waite, J. H.; Jensen, R. A.; Morse, D. E. *Biochemistry* **1992,** *31*, 5733–5738.

51 Zhao, H.; Sun, C.; Stewart, R. J.; Waite, J. H. *J. Biol. Chem.* **2005,** *280*, 42938–42944.

52 Stewart, R. J.; Weaver, J. C.; Morse, D. E.; Waite, J. H. *J. Exp. Biol.* **2004,** *207* (Pt 26), 4727–4734.

53 Kamino, K. *J. Adhes.* **2010,** *86*, 96–110.

54 Dalsin, J. L.; Hu, B. H.; Lee, B. P.; Messersmith, P. B. *J. Am. Chem. Soc.* **2003,** *125*, 4253–4258.

55 Saxer, S.; Portmann, C.; Tosatti, S.; Gademann, K.; Zuŕcher, S.; Textor, M. *Macromolecules* **2009,** *43*; 1050–1060.

56 Malisova, B.; Tosatti, S.; Textor, M.; Gademann, K.; Zuŕcher, S. *Langmuir* **2010,** *26*; 4018–4026.

57 Dalsin, J. L.; Lin, L.; Tosatti, S.; Voros, J.; Textor, M.; Messersmith, P. B. *Langmuir* **2005,** *21*, 640–646.

58 Westwood, G.; Horton, T. N.; Wilker, J. J. *Macromolecules* **2007,** *40*, 3960–3964.

59 McBride, M.; Wesselink, L. *Environ Sci. Technol.* **1988,** *22*, 703–708.

60 Connor, P.; Dobson, K.; McQuillan, A. *Langmuir* **1995,** *11*, 4193–4195.

61 Zhao, H.; Robertson, N. B.; Jewhurst, S. A.; Waite, J. H. *J. Biol. Chem.* **2006,** *281*, 11090–11096.

62 Vasudevan, D.; Stone, A. *Environ. Sci. Technol.* **1996,** *30*, 1604–1613.

63 Furubayashi, A.; Hiradate, S.; Fujii, Y. *J. Chem. Ecol.* **2007,** *33*, 239–250.

64 Lee, H.; Scherer, N. F.; Messersmith, P. B. *Proc. Natl. Acad. Sci. USA* **2006,** *103*, 12999–13003.

65 Wang, J.; Tahir, M.; Kappl, M.; Tremel, W.; Metz, N.; Barz, M., Theato, P.; Butt, H.-J. *Adv. Mater.* **2008,** *20*, 3872–3876.

66 Flammang, P.; Lambert, A.; Bailly, P.; Hennebert, E. *J. Adhes.* **2009,** *85*, 447–464.

67 Hui, S. Y.; Herve, A.; Kiplinger, J. *JCT Coatings Tech.* **2005,** *2*, 44–49.

68 de Majistre, R. U.S. Patent, PPG Industries Inc.: Pittsburgh, PA, 3,754,972, **1973.**

69 Janda, R.; Homburg, B.; Eppinger, B. U.S. Patent, Kulzer & Co.: GmbH Wehrheim, DE 4,640,936, **1987.**

70 Boothe, J.; Schaper, R. U.S. Patent, Calgon Corporation: Pittsburgh, PA, 4,650,591, **1987.**

71 Brovelli, D.; Hähner, G.; Ruiz, L.; Hofer, R.; Kraus, G.; Waldner, A., Schlösser, J.; Oroszlan, P.; Ehrat, M.; Spencer, N. D *Langmuir* **1999,** *15*, 4324–4327.

72 Marcinko, S.; Fadeev, A. *Langmuir* **2004,** *20*, 2270–2273.

73 Thissen, P.; Valtiner, M.; Grundmeier, G. *Langmuir* **2009,** *26*, 156–164.

74 Zoulalian, V.; Zuŕcher, S.; Tosatti, S.; Textor, M.; Monge, S.; Robin, J.-J. *Langmuir* **2010,** *26*, 74–82.

75 Chang, S. H.; Han, J. L.; Tseng, S. Y.; Lee, H. Y.; Lin, C. W.; Lin, Y. C., Jeng, W.-Y.; Wang, A. H.-J.; Wu, C.-Y.; Wong, C.-H. *J. Am. Chem. Soc.* **2010,** *132*, 13371–13380.

76 Elzinga, E.; Sparks, D. *J. Colloid Interface Sci.* **2007,** *308*, 53–70.

77 Rahnemaie, R.; Hiemstra, T.; van Riemsdijk, W. *Langmuir* **2007,** *23*, 3680–3689.

78 Tejedor-Tejedor, M.; Anderson, M. *Langmuir* **1990,** *6*, 602–611.

79 Connor, P.; McQuillan, A. *Langmuir* **1999,** *15*, 2916–2921.

80 Arai, Y.; Sparks, D. *J. Colloid Interface Sci.* **2001,** *241*, 317–326.

81 Di Blasi, C.; Geelhoed, J.; Hiemstra, T. *Geochim Cosmochim Acta* **1997;** *61*: 2389–2396(8).

82 Upritchard, H.; Yang, J.; Bremer, P.; Lamont, I.; McQuillan, A. *Langmuir* **2007,** *23*, 7189–7195.

83 Geelhoed, J.; Hiemstra, T.; Van Riemsdijk, W. *Geochim. Cosmochim. Acta* **1997,** *61*, 2389–2396.

84 Geelhoed, J.; Hiemstra, T.; Van Riemsdijk, W. *Environ. Sci. Technol.* **1998,** *32*, 2119–2123.

85 The pK_a values of amino acids can be shifted dramatically from their solution values by their local microenvironments.

86 Sundberg, R.; Martin, R. *Chem. Rev.* **1974,** *74*, 471–517.

87 Block, H.; Maertens, B.; Spriestersbach, A.; Brinker, N.; Kubicek, J.; Fabis, R., Labahn, J.; Schafer, F.. *Methods Enzymol.* **2009,** *463*, 439–473.

88 Szilagyi, I.; Labadi, I.; Hernadi, K.; Kiss, T.; Palinko, I. Montmorillonite Intercalated Cu(II)-Histidine Complex—Synthesis, Characterisation and Superoxide Dismutase Activity. Studies in Surface Science and Catalysis; Elsevier, **2005;** *158* pp 1011–1018.

89 Grommen, R.; Manikandan, P.; Gao, Y.; Shane, T.; Shane, J. J.; Schoonheydt, R. A., Weckhuysen, B. M.; Goldfarb, D. *J. Am. Chem. Soc.* **2000,** *122*, 11488–11496.

90 Vlasova, N. N.; Golovkova, L. P. *Colloid J.* **2004,** *66*, 657–662.

91 Roddick-Lanzilotta, A.; Connor, P.; McQuillan, A. *Langmuir* **1998,** *14*, 6479–6484.

92 Roddick-Lanzilotta, A.; McQuillan, A. *J. Colloid Interface Sci.* **1999,** *217*, 194–202.

93 Parbhakar, A.; Cuadros, J.; Sephton, M.; Dubbin, W.; Coles, B.; Weiss, D. *Colloids Surf A: Physicochem. Eng. Aspects* **2007,** *307*, 142–149.

94 Monti, S.; Walsh, T. R. *J. Phys. Chem. C* **2010,** *114*, 22197–22206.

95 Garcia-Ramos, J.; Carmona, P. *Can. J. Chem.* **1981,** *59*, 222–226.

96 Song, D.; Chen, M.; Liang, Y.; Bai, Q.; Chen, J.; Zheng, X. *Acta Biomater.* **2010,** *6*, 684–694.

97 Gerke, J. *Soil Sci.* **2010,** *175*, 417–425.

98 Boudou, T.; Crouzier, T.; Ren, K.; Blin, G.; Picart, C. *Adv. Mater.* **2010,** *22*, 441–467.

99 Bucur, C.; Sui, Z.; Schlenoff, J. *J. Am. Chem. Soc.* **2006,** *128*, 13690–13691.

100 Bharadwaj, S.; Montazeri, R.; Haynie, D. *Langmuir* **2006,** *22*, 6093–6101.

101 Waite, J. H.; Andersen, N. H.; Jewhurst, S.; Sun, C. *J. Adhes.* **2005,** *81*, 297–317.

102 Waite, J. H. *Results Probl. Cell Differ.* **1992,** *19*, 27–54.

103 Taylor, S. W.; Chase, D. B.; Emptage, M. H.; Nelson, M. J.; Waite, J. H. *Inorg. Chem.* **1996,** *35*, 7572–7577.

104 Monahan, J.; Wilker, J. J. *Chem. Commun.* (Camb) **2003,** *14*, 1672–1673.

105 An experimental caveat is the difficulty of exactly replicating the pH, salts, and salinity of the ocean in the SFA. However, the pH and ionic strength within the space created by the tip of the foot in which the plaque is formed is unknown and may differ significantly from the ocean and from the SFA experimental conditions.

106 Harrington, M. J.; Masic, A.; Holten-Andersen, N.; Waite, J. H.; Fratzl, P. *Science* **2010.**

107 Lin, Q.; Gourdon, D.; Sun, C.; Holten-Andersen, N.; Anderson, T. H.; Waite, J. H.; Israelachvili, J. N. *Proc. Natl. Acad. Sci. USA* **2007,** *104*, 3782–3786.

108 Hopkins, T. L.; Kramer, K. J. *Annu. Rev. Entomol.* **1992,** *37*, 273–302.

109 Hopkins, T. L.; Morgan, T. D.; Aso, Y.; Kramer, K. J. *Science* **1982,** *217*, 363–366.

110 Ito, S. *Pigment Cell Res.* **2003,** *16*, 230–236.

111 Lee, B. P.; Dalsin, J. L.; Messersmith, P. B. *Biomacromolecules* **2002,** *3*, 1038–1047.

112 McDowell, L. M.; Burzio, L. A.; Waite, J. H.; Schaefer, J. *J. Biol. Chem.* **1999,** *274*, 20293–20295.

113 Zhao, H.; Waite, J. H. *Biochemistry* **2005,** *44*, 15915–15923.

114 Zhao, H.; Waite, J. H. *J. Biol. Chem.* **2006,** *281*, 26150–26158.

115 Sever, M. J.; Weisser, J. T.; Monahan, J.; Srinivasan, S.; Wilker, J. J. *Angew. Chem. Int. Ed. Engl.* **2004,** *43*, 448–450.

116 Wilker, J. J. *Curr. Opin. Chem. Biol.* **2010,** *14*, 276–283.

117 Holten-Andersen, N.; Waite, J. H. *J. Dent. Res.* **2008,** *87*, 701–709.

118 Stevens, M. J.; Steren, R. E.; Hlady, V.; Stewart, R. J. *Langmuir* **2007,** *23*, 5045–5049.

119 Orci, L.; Ravazzola, M.; Anderson, R. *Nature* **1987,** *326*, 77–79.

120 Pace, C.; Sachs, G. *Am. J. Physiol. Cell Physiol.* **1982,** *242*, C382–C387.

121 Perez-Vilar, J.; Mabolo, R.; McVaugh, C.; Bertozzi, C.; Boucher, R. *J. Biol. Chem.* **2006,** *281*, 4844–4855.

122 Stewart, R. J.; Wang, C. S.; Shao, H. *Adv. Colloid Interface Sci.* **2010,** doi:10.1016/j.cis.2010.10.009.

123 Lim, S.; Choi, Y. S.; Kang, D. G.; Song, Y. H.; Cha, H. J. *Biomaterials* **2010,** *31*, 3715–3722.

124 Hwang, D. S.; Waite, J. H.; Tirrell, M. *Biomaterials* **2010,** *31*, 1080–1084.

125 Miyake, S.; Azuma, M. *J. Insect Biotechnol. Sericol.* **2008,** *77*, 9–16.

126 Terry, A.; Knight, D.; Porter, D.; Vollrath, F. *Biomacromolecules* **2004,** *5*, 768–772.

127 Symes, J. L.; Kester, D. R. *Marine Chem.* **1985,** *17*, 57–74.

128 Gordon, R. M.; Martin, J. H.; Knauer, G. A. *Nature* **1982,** *299*, 611–612.

129 Walker, G. *Marine Biol.* **1970,** *25*, 239–248.

130 Power, A. M.; Klepal, W.; Zheden, V.; Jonker, J.; McEvilly, P.; von Byern, J. In Mechanisms of Adhesion in Adult Barnacles; von Byern, J.; Grunwald, I., Eds.; Springer: New York, **2010.**

131 Walker, G. In Cirripedia; Harrison, F. W.; Humes, A. G., Eds.; Wiley-Liss: New York, **1992.**

132 Wiegemann, M. *Aquatic Sci. Res. Across Boundaries* **2005,** *67*, 166–176.

133 Sullan, R. M. A.; Gunari, N.; Tanur, A. E.; Chan, Y.; Dickinson, G. H.; Orihuel, B., Rittschof, D.; Walker, G. C. *Biofouling* **2009,** *25*, 263–275.

134 Barlow, D. E.; Dickinson, G. H.; Orihuela, B.; Kulp, J. L.; Rittschof, D.; Wahl, K. J. *Langmuir* **2010,** *26*, 6549–6556.

135 Nakano, M.; Shen, J.; Kamino, K. *Biomacromolecules* **2007,** *8*, 1830–1835.

136 Dickinson, G.; Vega, I.; Wahl, K.; Orihuela, B.; Beyley, V.; Rodriguez, E., Everett, R. K.; Bonaventura, J.; Rittschof, D. *J. Exp. Biol.* **2009,** *212*, 3499–3510.

137 Kamino, K. *Biofouling* **2010,** *26*, 755–760.

138 Despain, R.; De Vries, K.; Luntz, R.; Williams, M. *J. Dent. Res.* **1973,** *52*, 674–679.

139 Stewart, R. J. *Appl. Microbiol. Biotechnol.* **2011,** *89*, 27–33.

140 Statz, A.; Finlay, J.; Dalsin, J.; Callow, M.; Callow, J. A.; Messersmith, P. B. *Biofouling* **2006,** *22*, 391–399.

141 Fan, X.; Lin, L.; Messersmith, P. B. *Biomacromolecules* **2006,** *7*, 2443–2448.

142 Statz, A. R.; Meagher, R. J.; Barron, A. E.; Messersmith, P. B. *J. Am. Chem. Soc.* **2005,** *127*, 7972–7973.

143 Kang, S. M.; You, I.; Cho, W. K.; Shon, H. K.; Lee, T. G.; Choi, I. S.; Karp, J. M.; Lee, H. *Angew. Chem. Int. Ed. Engl.* **2010,** *49*, 9401–9404.

144 Brubaker, C. E.; Kissler, H.; Wang, L. J.; Kaufman, D. B.; Messersmith, P. B. *Biomaterials* **2010,** *31*, 420–427.

145 Lee, H.; Lee, B. P.; Messersmith, P. B. *Nature* **2007,** *448*, 338–341.

146 Holten-Andersen, N.; Harrington, M. J.; Birkedal, H.; Lee, B. P.; Messersmith, P. B.; Lee, K. Y. C.; Waite, J. H. *Proc. Natl. Acad. Sci. USA*, **2011,** *108*, 2651–2655.

147 Shao, H.; Stewart, R. J. *Adv. Mater.* **2010,** *22*, 729–733.

148 Shao, H.; Bachus, K. N.; Stewart, R. J. *Macromol. Biosci.* **2009,** *9*, 464–471.

149 Winslow, B. D.; Shao, H.; Stewart, R. J.; Tresco, P. A. *Biomaterials* **2010,** *31*, 9373–9381.

150 Kaur, S.; Weerasekare, G. M.; Stewart, R. J. *ACS Appl. Mater. Interfaces*, in press; Doi: 10.1021/am200082v.

151 Flammang, P.; Santos, R.; Haesaerts, D. *Prog. Mol. Subcell Biol.* **2005,** *39*, 201–220.

152 Burkett, J.; Hight, L.; Kenny, P. *J. Am. Chem. Soc.* **2010,** *132*, 12531–12533.